SCIENCE CHINA
Chemistry

• ARTICLES •

November 2016 Vol.59 No.11: 1486–1491
doi: 10.1007/s11426-016-0103-7

Quantum dots protect against MPP^+-induced neurotoxicity in a cell model of Parkinson's disease through autophagy induction

Lu Wang[1†], Xiaoming Li[1,4†], Yuping Han[2], Ting Wang[2], Yun Zhao[2*], Aldalbahi Ali[3], Nahed Nasser El-Sayed[3], Jiye Shi[5], Wenfeng Wang[1], Chunhai Fan[1] & Nan Chen[1*]

[1]*Division of Physical Biology and Bioimaging Center, Shanghai Synchrotron Radiation Facility, CAS Key Laboratory of Interfacial Physics and Technology, Shanghai Institute of Applied Physics, Chinese Academy of Sciences, Shanghai 201800, China*
[2]*School of Life Science, Sichuan University, Chengdu 610064, China*
[3]*Chemistry Department, King Saud University, Riyadh 11451, Saudi Arabia*
[4]*School of Life Science and Technology, ShanghaiTech University, Shanghai 201210, China*
[5]*UCB Pharma, Slough, SL1 3WE, UK*

Received March 9, 2016; accepted April 28, 2016; published online October 17, 2016

Autophagy is a basic cellular process that decomposes damaged organelles and aberrant proteins. Dysregulation of autophagy is implicated in pathogenesis of neurodegenerative disorders, including Parkinson's disease (PD). Pharmacological compounds that stimulate autophagy can provide neuroprotection in models of PD. Nanoparticles have emerged as regulators of autophagy and have been tested in adjuvant therapy for diseases. In this present study, we explore the effects of quantum dots (QDs) that can induce autophagy in a cellular model of Parkinson's disease. CdTe/CdS/ZnS QDs protect differentiated rat pheochromocytoma PC12 cells from MPP^+-induced cell damage, including reduced viability, apoptosis and accumulation of α-Synuclein, a characteristic protein of PD. The protective function of QDs is autophagy-dependent. In addition, we investigate the interaction between quantum dots and autophagic pathways and identify beclin1 as an essential factor for QDs-induced autophagy. Our results reveal new promise of QDs in the theranostic of neurodegenerative diseases.

quantum dots, autophagy, Parkinson's disease, α-Synuclein, Beclin1

Citation: Wang L, Li X, Han Y, Wang T, Zhao Y, Ali A, El-Saued NN, Shi J, Wang W, Fan C, Chen N. Quantum dots protect against MPP^+-induced neurotoxicity in a cell model of Parkinson's disease through autophagy induction. *Sci China Chem*, 2016, 59:1486−1491, doi: 10.1007/s11426-016-0103-7

1 Introduction

Due to their unique physicochemical properties, quantum dots (QDs) have shown great promise in many biomedical applications that include bioimaging, drug-delivery and photodynamic therapy [1–3]. However, practical applications of QDs in biomedicine have been largely restricted by concerns about their nanotoxicity [4,5]. Tremendous efforts have been made to improve the biosafety of QDs [6,7]. For example, effective coating of CdTe QDs with core-shell-shell (CSS) structures (i.e., CdTe/CdS/ZnS QDs) prevented the release of cadmium ions and greatly reduced their cytotoxicity [8,9]. More recently, we illustrated an autophagy-dependent mechanism that enhanced the Cd^{2+}-induced cytotoxicity of QDs. It is noteworthy that CSS QDs-induced autophagy, if not combined with other toxic factors, does not impair cell viability or functionality [10]. Recently, QDs with stable out surface layers were synthesized and appeared to be biocompatible in cell culture or in model organisms [11–13]. Nevertheless, autophagy induced by QDs has not been explored for therapeutical applications.

†These authors contributed equally to this work.
*Corresponding authors (email: zhaoyun@scu.edu.cn; chennan@sinap.ac.cn)

© Science China Press and Springer-Verlag Berlin Heidelberg 2016

Parkinson's disease (PD) is one of the most common neurodegenerative disorders. Although the pathogenesis of PD remains elusive, mitochondrial dysfunction and oxidative stress clearly contribute to the onset of this disease [14,15]. PD is associated with the accumulation of α-Synuclein protein aggregates, which is the major component of Lewy bodies in sporadic PDs [16]. α-Synuclein is degraded by both proteasome and autophagy [17]. Recently, malfunction of autophagy has been directly linked to a growing number of neurodegenerative disorders including PD, indicating the pivotal role of autophagy in neuronal homeostasis. Autophagy is a catabolic process that removes altered or misfolded proteins. Due to its essential role in clearance of pathogenic protein aggregates, autophagy has become an emerging target for the treatment of Parkinson's disease [18,19]. For example, stimulation of autophagy by rapamycin enhances the clearance of α-Synuclein and delays onset of Parkinson's or Alzheimer's disease [14,20]. Therefore, it is urgent to develop new approaches that regulate the signaling pathways of autophagy for the treatment of neurodegenerative diseases. Meanwhile, autophagy can be also considered as an alternative route for the degradation of misfolded proteins such as Huntingtin protein and amyloid-beta polypeptide [21–23]. Therefore, it is urgent to develop new approaches that regulate the signaling pathways of autophagy for the treatment of neurodegenerative diseases.

With the rapid development of nanotechnology, a growing number of nanoparticles have been reported as stimulators of autophagy both *in vitro* and *in vivo* [18–20]. However, effects of nanoparticles-induced autophagy on the progression of neurodegenerative diseases have barely been studied [21]. Recently, rare earth oxide nanoparticles have been demonstrated to induce autophagy and accelerate the clearance of mutant Huntingtin protein [22,23]. In this present study, we investigated the cellular effects of autophagy-inducing QDs in an MPP^+-induced cellular model of Parkinson's disease and underlying mechanism.

2 Experimental

2.1 Cell line, reagents and antibodies

Differentiated rat pheochromocytoma (PC12) cell line was purchased from Shanghai Institute of Cell Biology, Chinese Academy of Sciences (Shanghai, China). Dulbecco's modified Eagle medium (DMEM), fetal bovine serum (FBS), 2′,7′-dichlorofluorescin diacetate (DCFH-DA) and Caspase-3 activity assay kit were obtained from Invitrogen (USA). Thiazolyl blue tetrazolium bromide (MTT), MPP^+ iodide salt, rapamycin, 3-MA, sodium dodecyl sulfate (SDS) and hoechst 33258 were from Sigma-Aldrich (USA). Primary antibodies against α-Synuclein and Actin were from Abcam (Cambridge, UK). Primary antibody against LC3 was purchased from Cell Signaling Technology (USA). HRP conjugated anti-rabbit secondary antibody and fluorescein isothiocyanate (FITC)-labeled goat anti-rabbit secondary antibody were purchased from KPL (USA). ECL plus and poly(vinylidene fluoride) (PVDF) membrane were purchased from Millipore (USA). Fluorescence mounting medium was obtained from DAKO (Denmark). All pure analytical grade chemical reagents were obtained from Sinopharm (China).

2.2 Preparation of CdTe and CdTe/CdS/ZnS QDs

The water-dispersed CdTe QDs and CdTe/CdS/ZnS QDs were synthesized as previously reported [7].

2.3 Cell culture and treatment

PC12 cells were cultured in DMEM supplemented with 10% (*v*/*v*) heat-inactivated FBS, and antibiotics (100 μg/mL treptomycin and 100 U/mL penicillin) at 37 °C in the humidified atmosphere with 5% CO_2. For PD model cells, PC12 cells were incubated with 2 μM MPP^+ for 48 h. 75 nM CSS QDs were added 6 h before MPP^+ incubation.

2.4 Cell viability determination via MTT assay

Cell viability was determined by MTT assay. In brief, cells were seeded in 96-well plates and incubated overnight. After various treatments, cells were incubated with 20 μL MTT solution (5 mg/mL) for 4 h at 37 °C. Cells were then lysed with 10% SDS in 0.01 M HCl (pH 2–3), solubilizing the formazan crystals. After centrifugation, the absorbance of supernatant was measured at 570 nm using a microplate reader (Bio-Rad 680, USA).

2.5 Western blot analysis

PC12 cells were plated using 6-well plates before treatment. Cells were harvested in SDS-loading sample buffer and boiled. Protein samples were then analyzed by 12% SDS-polyacrylamide gelelectrophoresis (SDS-PAGE) and blotted to PVDF membranes. The blots were blocked with 5% nonfat dry milk dissolved in PBST buffer (PBS+0.1% Tween 20, PBS=phosphate buffer saline) for 30 min and then incubated overnight with desired primary antibodies at 4 °C. After washing with PBST, the blots were probed with a goat anti-rabbit HRP secondary antibody for 1 h at room temperature. Next, the membranes were visualized using the chemiluminescent HRP substrate method (Millipore) and the representative bands of proteins were measured with a bio-imaging system (Syngene G: Box).

2.6 Immunofluorescence staining

Cells cultured on coverslips were fixed in 4% paraformal-

dehyde for 20 min. After being washed by PBS for 3 times, cells were incubated with blocking solution (1% BSA in PBS) for 30 min, followed by incubation with α-Synuclein primary antibody (1:200) for 1 h at room temperature. After being washed with PBS, cells were treated with FITC-labeled secondary antibody for another 1 h. Coverslips were then washed again and mounted using DAKO fluorescence mount (Denmark). Images were acquired using a laser confocal microscope (Leica TCS SP8, Germany).

2.7 Measurement of intracellular ROS

Intracellular reactive oxygen species (ROS) levels were detected with 2′,7′-dichlorofluorescin diacetate (DCFH-DA). Cells were firstly incubated with 10×10^{-6} M DCFH-DA for 10 min. Fluorescence intensity was measured using a fluorimeter (495 nm excitation/520 nm emission; Bio-Rad 680, USA).

2.8 Caspase-3 activity determination

The activity of Caspase-3 was determined using the Caspase-3 activity kit (Beyotime, China) according to the manufacturer's protocol. A reaction mixture of 10 μL cell lysate, 80 μL reaction buffer (20 mM Tris-HCl, pH 7.5, 1% NP-40) and 10 μL Caspase-3 substrate (Ac-DEVD-pNA) (2 mM) was prepared and incubated at 37 °C for 4 h. Absorbance at 405 nm was measured using a microplate reader (Bio-Rad 680). Average percentage and standard deviations of three biological replicates are shown.

2.9 siRNA transfection

Transfections were carried out approximately 24 h after seeding, using the Amaxa electroporation system (Lonza, Cologne AG, Belgium). PC12 cells were collected and resuspended in Nucleofector solution and mixed with 1.5 μg $siRNA^{Beclin1}$ (5′-AACUCAGGAGAGGAGCCAUUU-3′) or $siRNA^{Ctrl}$ (5′-UUCUCCGAACGUGUCACGU-3′). Further analysis was performed 24 h after electroporation.

2.10 Quantitative PCR

Total RNA was isolated using Trizol reagent according to the manufacturer's protocol. For cDNA synthesis, Superscript III First-Strand Synthesis system (Invitrogen, USA) was used. Quantitative real time polymerase chain reaction (RT-PCR) was performed using the StepOnePlus™ Real-Time PCR Systems (Applied Biosystems, USA). Following primer sequences were used: 5′-CGGCTCCTATTCCATCAAAA-3′ and 5′-AAGCAAGACCCCACTTGAGA-3′ for Beclin1 and 5′-TCCACAGAAAGTGCCAACAG-3′ and 5′-TTCAGTCTTCGGCTGAGGTT-3′ for Actin. Average mRNA levels and standard deviations of at least two biological replicates are shown.

2.11 Statistical analysis

In all experiments, significance was determined using the Student's *t*-distribution (two-tailed; two-sample equal variance). *** equals $P<0.001$; ** equals $P<0.01$; * equals $P<0.05$; ns: not significant.

3 Results and discussion

3.1 QDs induce autophagy in a cell model of Parkinson's disease

Both CdTe and CdTe/CdS/ZnS (CSS) quantum dots can efficiently induce autophagy in differentiated rat pheochromocytoma PC12 cells [7]. We chose CSS QDs instead of CdTe QDs in the following experiment because of their superior biocompatibility. CSS QDs did not affect cell viability at a rather high concentration of 300 nM; while CdTe QDs showed potent dose-dependent inhibition of cell viability (Figure S1, Supporting Information online). Cell types and physiopathological changes can both influence the intracellular fate and biological effect of endocytotic nanoparticles [9,20]. For example, many nanomaterials exhibited anti-tumor effects without affecting normal cells [24]. To investigate the effects of QDs on PD model cells, we firstly examined whether QDs preserved their capacity to induce autophagy in pathological cells. 1-Methyl-4-phenyl-1,2,3,6-tetrahydropyridine (MPTP) is a neurotoxin and can selectively damage DA neurons, which in turn leads to clinical symptoms similar to those of patients with PD. Its metabolite MPP^+ induces mitochondrial dysfunction that mediates autophagy-lysosome pathway impairments in neurons. MPP^+ has been widely used to induce neurotoxicity in PC12 cells and model PD in cells [25]. Indeed, we observed that MPP^+ caused dose-dependent damages in PC12 cells (Figure S2). Incubation with 2 μM MPP^+ for 48 h induced a 5-fold reduction of metabolic activity (Figure 1(a)) and a 10-fold increase of intracellular reactive oxygen species (ROS) levels in PC12 cells (Figure 1(b)). Consistent with these observations, apoptosis was induced by MPP^+ treatment, as indicated by a 8-fold increase in Caspase-3 activity (Figure 1(c)). More importantly, MPP^+ significantly increased the levels of the α-Synuclein, the pathological hallmark of PD. Accumulation of α-Synuclein was demonstrated by immunofluorescent staining (Figure 1(d)) and immunoblotting (Figure 1(e)). Collectively, we developed Parkinson's disease cell model successfully by MPP^+ treatment.

We then examined the effects of MPP^+ and QDs co-treatment on the autophagic activity. The formation of double-membrane structured autophagosome is an essential hallmark of autophagy induction. Microtubule-associated protein light chain 3 (LC3) is the most widely used marker of autophagosomes [26]. However, LC3-II accumulation

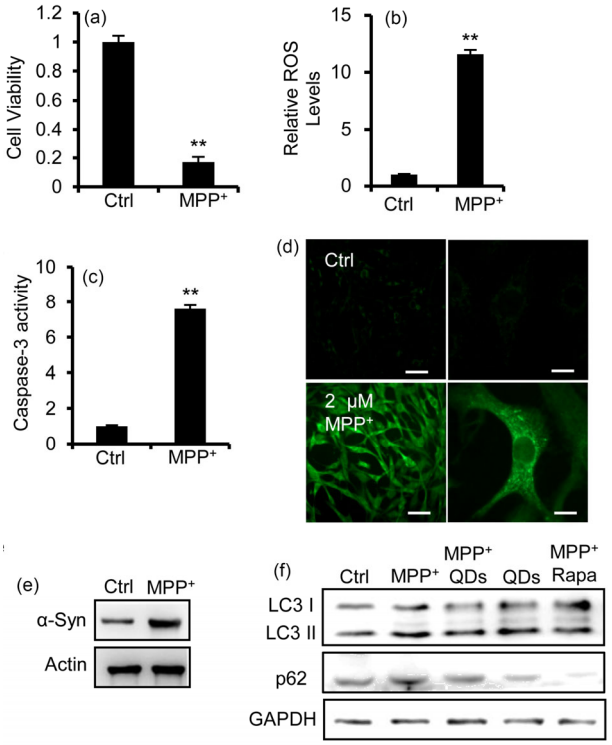

Figure 1 QDs induce autophagy in a cell model of Parkinson's disease. PC12 cells were incubated with 2 μM MPP^+ for 48 h and analyzed for (a) cell viability by MTT assay, (b) ROS levels by DCF staining, (c) Caspase-3 activity. α-Synuclein levels were monitored by (d) immunostaining and (e) immunoblotting. (f) PC12 cells were pre-incubated with 75 nM CSS QDs or 100 μM rapamycin for 6 h before MPP^+ treatment. Protein levels of LC3 II and p62 were analyzed by immunoblotting. Actin was included as loading control (color online).

occurs not only in autophagy induction, but also in a reduction in downstream degradation of autophagosome [27]. Therefore, we completed the LC3 analysis with assays to estimate overall autophagic flux. p62 is a target protein of autophagy and its degradation is a sign of complete autophagic flux [28]. We observed an increase in both LC3-II and p62 protein levels in MPP^+-treated cells (Figure 1(f)), suggesting that MPP^+ interfered the autophagic flux and blocked the degradation of p62. Pretreatment with CSS QDs restored the p62 levels to a similar extend of that in cells pretreated with rapamycin, a well-established autophagy stimulator. These results proved the capacity of QDs to induce autophagy in MPP^+-induced cell model of Parkinson's disease.

3.2 QDs protected PC12 cells from MPP^+-induced toxicity through autophagy induction

It is generally acknowledged that accumulation of misfolded or damaged proteins is detrimental to cell survival and function. For example, mutant α-Synuclein was reported to enhance the toxicity of MPP^+ in PC12 cells by increasing intracellular reactive oxygen species (ROS) [29]. Since we observed attenuated p62 accumulation in cells pre-treated with QDs, we wondered whether such enhanced clearance could antagonize MPP^+-induced toxicity. Indeed, cell viability, as measured by cell proliferation assay, was partially restored by QDs (Figure 2(a)). Consistently, ROS levels were also mitigated by QDs (Figure 2(b)). We also monitored the effects of QDs on MPP^+-induced apoptosis. Caspase-3 activities of cells co-treated with MPP^+ and QDs decreased dramatically relative to that of cells incubated with MPP^+ alone (Figure 2(c)), indicating that QDs could prevent MPP^+-treated PC12 cells from apoptosis. Importantly, protein levels of α-Synuclein were significantly reduced in cells incubated with both QDs and MPP^+ (Figure 2(d)). Taken together, our results demonstrated that QDs protected PC12 cells from MPP^+-caused damage, including cell growth inhibition, high levels of intracellular ROS, apoptosis and accumulation of neurotoxic α-Synuclein protein.

It has been reported that autophagy played an important role in degradation of aggregated α-Synuclein, and several types of autophagy activators have proven to alleviate MPP^+-induced neurotoxicity [17,22]. Therefore we assumed that the protective function of QDs depended on their ability to induce autophagy. To prove this, we blocked QDs-induced autophagy by pre-incubating cells with 3-methyladenine (3-MA), which inhibits autophagy by blocking initial steps in autophagosome formation via the inhibition of class III PI3K [30]. Indeed, 3-MA pretreatment abolished LC3-II accumulation, indicating inhibition of autophagy, which in turn caused high levels of α-Synuclein protein, both in the presence and absence of MPP^+ (Figure 3(a)). Furthermore, cell viability correlated well with the efficiency of autophagy. Neither QDs nor 3-MA affected viability of PC12 cells without MPP^+. However, 3-MA abolished the rescue effects

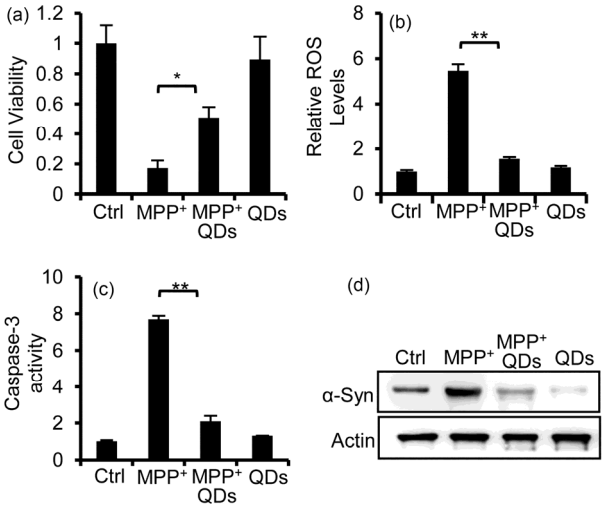

Figure 2 QDs rescue PC12 cells from MPP^+-induced cell damage. PC12 cells were incubated with 75 nM CSS QDs for 6 h before MPP^+ treatment and analyzed for (a) cell viability by MTT assay, (b) ROS levels by DCF staining, (c) Caspase-3 activity, (d) protein levels of α-Synuclein were monitored by immunoblotting.

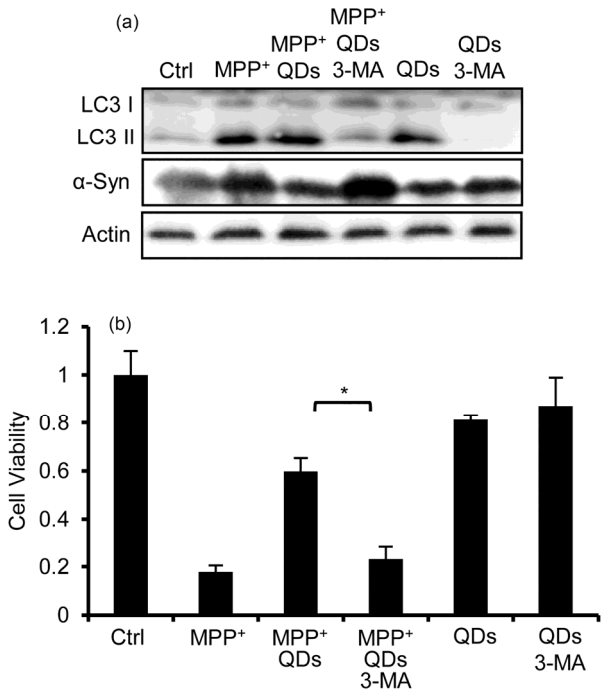

Figure 3 The protective effects of QDs are autophagy-dependent. MPP^+ and QDs-treated PC12 cells were incubated in the presence or absence of 5 mM 3-MA for 6 h and analyzed for: (a) protein levels of LC3-II and α-Synuclein by immunoblotting; (b) cell viability by MTT assay.

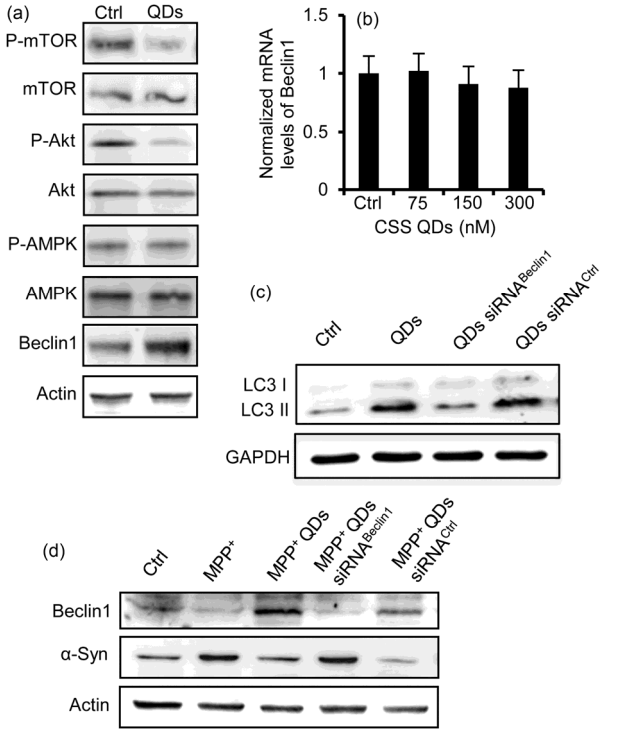

Figure 4 Beclin1 is required for QDs-induced autophagy. (a) PC12 cells were incubated with 75 nM CSS QDs for 24 h. Cell lysates were analyzed for the levels of indicated proteins by immunoblotting. (b) PC12 cells were incubated with indicated concentrations of CSS QDs for 24 h. mRNA levels of Beclin1 were determined by RT-PCR and normalized to mRNA levels of Actin. (c) Pre-treatment with $siRNA^{Beclin1}$ for 24 h inhibited QDs-induced autophagy. (d) QDs-induced degradation of α-Synuclein was abolished by siRNA-mediated knockdown of Beclin1.

of QDs in the MPP^+-induced PD model cells (Figure 3(b)). Hence CSS QDs protected against MPP^+-induced neurotoxicity through autophagy enhancement.

3.3 Beclin1 is required for QDs-induced autophagy

Next we investigated the mechanism of the protective role of QDs in PD cell model. Despite numerous studies about nanoparticles-induced autophagy, the underlying molecular mechanism is largely elusive [31,32]. Since regulation mechanisms and signaling pathways of autophagy were extensively studied, we probed the phosphorylation status of key proteins in autophagic signaling upon QDs treatment. The mammalian target of rapamycin (mTOR) complex is the master regulator of autophagy. Inhibition of mTOR induces autophagy [26]. Similar to rapamycin or starvation, QDs decreased levels of phosphorylated mTOR but had no effects on total mTOR protein levels, confirming QDs-induced autophagy was mTOR-dependent (Figure 4(a)). Then we examined two major upstream signaling pathways of mTOR. According to the phosphorylation/activation status measured by western blot, AKT pathway but not AMPK pathway was involved in QDs inhibition of mTOR. In addition, we observed up-regulation in protein levels of Beclin1 in QDs-treated cells (Figure 4(a)). Beclin1 plays an essential role in the nucleation and assembly of the initial phagophore membrane. Beclin1 dysfunction has been implicated in many disorders, including neurodegeneration [33,34]. We checked the mRNA levels of Beclin1, which were not changed by QDs treatment, implying that QDs increased the expression or stability of Beclin1 protein instead of its gene transcription (Figure 4(b)). To verify the indispensability of Beclin1 in QDs-induced autophagy, RNA interference was performed to knock down expression levels of Beclin1. Down-regulation of Beclin1 did inhibit QDs-induced accumulation of LC3-II, which confirmed that autophagy induced by QDs was Beclin1-dependent (Figure 4(c)). Moreover, the protective role of QDs in PD model cells also required Beclin1. The clearance of α-Synuclein aggregates by QDs was inhibited in the $siRNA^{Beclin1}$ treated PC12 cells (Figure 4(d)). Our data suggested that QDs-induced autophagy was Beclin1-dependent, and RNA interference-mediated knockdown of Beclin1 suppressed autophagy as well as the clearance of neurotoxic α-Synuclein (Figure 5).

4 Conclusions

Here, we established an *in vitro* Parkinson's disease model using MPP^+-injured PC12 cells to investigate the protective effects of CSS quantum dots. Autophagy-mediated clearance of aberrant α-Synuclein aggregates has been implicated

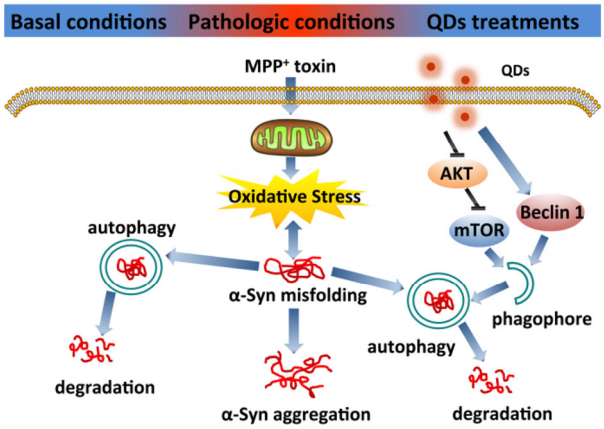

Figure 5 Scheme illustration of neuroprotective effects of CSS QDs in Parkinson's disease (PD) model cells. MPP^+ inhibited mitochondrial function and increased ROS levels, resulting in accumulation of neurotoxic α-Synuclein aggregates. CSS QDs induced autophagy by increasing protein levels of Belcin1 as well as inhibition of the AKT/mTOR signaling pathway. Up-regulation of autophagy accelerated the clearance of α-Synuclein and alleviated MPP^+-induced cell damage (color online).

in many neurodegenerative diseases including PD [35]. Pre-treatment with QDs significantly attenuated MPP^+-induced cell injury, including decreased viability, increased oxidative stress and apoptosis. QDs also inhibited MPP^+-induced accumulation of α-Synuclein. Our results proved that the protective role of QDs largely depended on their ability to stimulate autophagy, as evidenced by the inhibition of both autophagy and protective effects by 3-MA that blocked the initiation of autophagic process. In addition, we explored the mechanism of QDs-induced autophagy and identified Beclin1 as a key regulator. By using specific targeted small interfering RNA (siRNA) to knockdown the expression of Beclin1 protein, we observed that QDs-induced inhibition of MPP^+ stress was abolished. Our study suggested a potential beneficial purpose of autophagy-stimulation by QDs and many other nanoparticles in PD and related neuronal damage.

Acknowledgments This work was supported by the National Natural Science Foundation of China (U1332119, 31371015, 31470970), the Youth Innovation Promotion Association, CAS (2015211), Visiting Professor Program at King Saud University and the Shanghai Municipal Commission for Science and Technology (13NM1402300). We would like to dedicate this paper to Professor Qing Huang, who unfortunately passed away during the manuscript preparation process.

Conflict of interest The authors declare that they have no conflict of interest.

Supporting information The supporting information is available online at http://chem.scichina.com and http://link.springer.com/journal/11426. The supporting materials are published as submitted, without typesetting or editing. The responsibility for scientific accuracy and content remains entirely with the authors.

1 Wu C, Shi L, Wu C, Guo D, Selke M, Wang X. *Sci China Chem*, 2014, 57: 1579–1588
2 Hou S, Liang L, Deng S, Chen J, Huang Q, Cheng Y, Fan C. *Sci China Chem*, 2014, 57: 100–106
3 Markovic ZM, Ristic BZ, Arsikin KM, Klisic DG, Harhaji-Trajkovic LM, Todorovic-Markovic BM, Kepic DP, Kravic-Stevovic TK, Jovanovic SP, Milenkovic MM, Milivojevic DD, Bumbasirevic VZ, Dramicanin MD, Trajkovic VS. *Biomaterials*, 2012, 33: 7084–7092
4 Winnik FM, Maysinger D. *Accounts Chem Res*, 2013, 46: 672–680
5 Wu T, Zhang T, Chen Y, Tang M. *J Appl Toxicol*, 2016, 36: 345–351
6 Chen N, He Y, Su YY, Li XM, Huang Q, Wang HF, Zhang XZ, Tai RZ, Fan CH. *Biomaterials*, 2012, 33: 1238–1244
7 Li XM, Chen N, Su YY, He Y, Yin M, Wei M, Wang LH, Huang W, Fan CH, Huang Q. *Adv Healthc Mater*, 2014, 3: 354–359
8 Zhou Y, Wang Q, Song B, Wu S, Su Y, Zhang H, He Y. *Biomaterials*, 2015, 72: 38–48
9 Tsoi KM, Dai Q, Alman BA, Chan WC. *Accounts Chem Res*, 2013, 46: 662–671
10 Yong KT, Law WC, Hu R, Ye L, Liu L, Swihart MT, Prasad PN. *Chem Soc Rev*, 2013, 42: 1236–1250
11 Bove J, Martinez-Vicente M, Vila M. *Nat Rev Neurosci*, 2011, 12: 437–452
12 Tian T, Zhang JC, Lei HZ, Ying Z, Shi JY, Hu J, Huang Q, Fan CH, Sun YH. *Nucl Sci Technol*, 2015, 26: 100–105
13 Winslow AR, Chen CW, Corrochano S, Acevedo-Arozena A, Gordon DE, Peden AA, Lichtenberg M, Menzies FM, Ravikumar B, Imarisio S, Brown S, O'Kane CJ, Rubinsztein DC. *J Cell Biol*, 2010, 190: 1023–1037
14 Xilouri M, Vogiatzi T, Vekrellis K, Stefanis L. *Autophagy*, 2008, 4: 917–919
15 Liu K, Huang J, Chen R, Zhang T, Shen L, Yang J, Sun X. *Braz J med Biol Res*, 2012, 45: 401–407
16 Lipinski MM, Zheng B, Lu T, Yan ZY, Py BF, Ng A, Xavier RJ, Li C, Yankner BA, Scherzer CR, Yuan JY. *Proc Natl Acad Sci USA*, 2010, 107: 14164–14169
17 Renna M, Jimenez-Sanchez M, Sarkar S, Rubinsztein DC. *J Biol Chem*, 2010, 285: 11061–11067
18 Zabirnyk O, Yezhelyev M, Seleverstov O. *Autophagy*, 2007, 3: 278–281
19 Yu L, Lu Y, Man N, Yu SH, Wen LP. *Small*, 2009, 5: 2784–2787
20 Khan MI, Mohammad A, Patil G, Naqvi SAH, Chauhan LKS, Ahmad I. *Biomaterials*, 2012, 33: 1477–1488
21 Zhang YJ, Zheng F, Yang TL, Zhou W, Liu Y, Man N, Zhang L, Jin N, Dou QQ, Zhang Y, Li ZQ, Wen LP. *Nat Mater*, 2012, 11: 817–826
22 Wei PF, Zhang L, Nethi SK, Barui AK, Lin J, Zhou W, Shen Y, Man N, Zhang YJ, Xu J, Patra CR, Wen LP. *Biomaterials*, 2014, 35: 899–907
23 Wei PF, Jin PP, Barui AK, Hu Y, Zhang L, Zhang JQ, Shi SS, Zhang HR, Lin J, Zhou W, Zhang YJ, Ruan RQ, Patra CR, Wen LP. *Biomaterials*, 2015, 73: 160–174
24 Wei PF, Zhang L, Lu Y, Man N, Wen LP. *Nanotechnology*, 2010, 21: 1–11
25 Hung KC, Huang HJ, Lin MW, Lei YP, Lin AM. *PLoS One*, 2014, 9: e91074
26 He C, Klionsky DJ. *Annu Rev Genet*, 2009, 43: 67–93
27 Zhong WY, Min L, Liu LY, Sun JL, Zhong ZT, Zhao Y, Song HY. *Chin Sci Bull*, 2013, 58: 4031–4038
28 Klionsky DJ, Abeliovich H, Agostinis P, et al. *Autophagy*, 2008, 4: 151–175
29 Dadakhujaev S, Noh HS, Jung EJ, Cha JY, Baek SM, Ha JH, Kim DR. *Neurosci Lett*, 2010, 472: 47–52
30 Ronan B, Flamand O, Vescovi L, Dureuil C, Durand L, Fassy F, Bachelot MF, Lamberton A, Mathieu M, Bertrand T, Marquette JP, El-Ahmad Y, Filoche-Romme B, Schio L, Garcia-Echeverria C, Goulaouic H, Pasquier B. *Nat Chem Biol*, 2014, 10: 1013–1019
31 Luo YH, Wu SB, Wei YH, Chen YC, Tsai MH, Ho CC, Lin SY, Yang CS, Lin P. *Chem Res Toxicol*, 2013, 26: 662–673
32 Zhang Y, Wang Z, Li X, Wang L, Yin M, Wang L, Chen N, Fan C, Song H. *Adv Mater*, 2015, 28: 1387–1393
33 Spencer B, Potkar R, Trejo M, Rockenstein E, Patrick C, Gindi R, Adame A, Wyss-Coray T, Masliah E. *J Neurosci*, 2009, 29: 13578–13588
34 Wang RC, Wei Y, An Z, Zou Z, Xiao G, Bhagat G, White M, Reichelt J, Levine B. *Science*, 2012, 338: 956–959
35 Wong E, Cuervo AM. *Nat Neurosci*, 2010, 13: 805–811